

# Scope and Mechanistic Analysis of the Enantioselective Synthesis of Allenes by Rhodium-Catalyzed Tandem Ylide Formation/[2,3]-Sigmatropic Rearrangement between Donor/Acceptor Carbenoids and Propargylic Alcohols

Zhanjie Li,<sup>†</sup> Vyacheslav Boyarskikh,<sup>†,‡</sup> Jørn H. Hansen,<sup>†</sup> Jochen Autschbach,<sup>§</sup> Djamaladdin G. Musaev,<sup>‡</sup> and Huw M. L. Davies<sup>\*,†</sup>

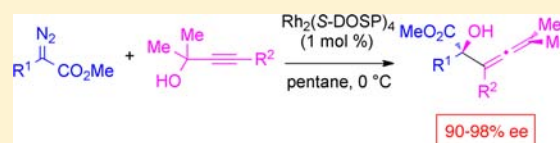
<sup>†</sup>Department of Chemistry, Emory University, 1515 Dickey Drive, Atlanta, Georgia 30322, United States

<sup>‡</sup>Cherry L. Emerson Center for Scientific Computation, Emory University, 1521 Dickey Drive, Atlanta, Georgia 30322, United States

<sup>§</sup>Department of Chemistry, University at Buffalo, The State University of New York, Buffalo, New York 14260, United States

## S Supporting Information

**ABSTRACT:** Rhodium-catalyzed reactions of tertiary propargylic alcohols with methyl aryl- and styryldiazoacetates result in tandem reactions, consisting of oxonium ylide formation followed by [2,3]-sigmatropic rearrangement. This process competes favorably with the standard O–H insertion reaction of carbenoids. The resulting allenenes are produced with high enantioselectivity (88–98% ee) when the reaction is catalyzed by the dirhodium tetraproline complex, Rh<sub>2</sub>(S-DOSP)<sub>4</sub>. Kinetic resolution is possible when racemic tertiary propargylic alcohols are used as substrates. Under the kinetic resolution conditions, the allenenes are formed with good diastereoselectivity and enantioselectivity (up to 6.1:1 dr, 88–93% ee), and the unreacted alcohols are enantioenriched to 65–95% ee. Computational studies reveal that the high asymmetric induction is obtained via an organized transition state involving a two-point attachment: ylide formation between the alcohol oxygen and the carbenoid and hydrogen bonding of the alcohol to a carboxylate ligand. The 2,3-sigmatropic rearrangement proceeds through initial cleavage of the O–H bond to generate an intermediate with close-lying open-shell singlet, triplet, and closed-shell singlet electronic states. This intermediate would have significant diradical character, which is consistent with the observation that the 2,3-sigmatropic rearrangement is favored with donor/acceptor carbenoids and more highly functionalized propargylic alcohols.

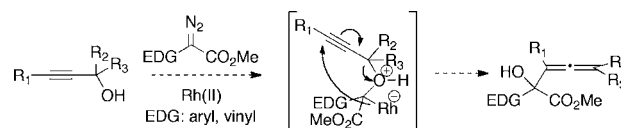


## INTRODUCTION

Metal–carbenoid insertions into X–H bonds (X = C, O, N, etc.) have been extensively studied over the last few decades.<sup>1</sup> In particular, metal–carbenoid insertions into O–H bonds have received considerable attention as an effective method for the synthesis of  $\alpha$ -alkoxy and  $\alpha$ -hydroxy carbonyl compounds, which are important motifs in natural products and pharmaceutical targets.<sup>2</sup> These O–H insertion reactions are believed to proceed, mechanistically, via formation of an oxonium ylide followed by a proton transfer. Although some chiral copper catalysts result in O–H insertion with high levels of asymmetric induction, in general no asymmetric induction is observed in rhodium-catalyzed reactions.<sup>3,4</sup>

Recently, we discovered that the rhodium(II)-catalyzed reactions of donor/acceptor carbenoids with highly substituted allyl alcohols do not lead to O–H insertion products.<sup>5,6</sup> Instead, a tandem oxonium ylide formation/[2,3]-sigmatropic rearrangement process occurs. The discovery of this new unexpected reaction pathway between carbenoids and alcohols has prompted us to explore the reactions of donor/acceptor carbenoids with propargylic alcohols. A similar tandem oxonium ylide formation/[2,3]-sigmatropic rearrangement would generate  $\alpha$ -hydroxy allenenes (Scheme 1).<sup>7</sup> Herein, we

## Scheme 1. Proposed Tandem Oxonium Ylide Formation/[2,3]-Sigmatropic Rearrangement



report the results of this study, which includes both experimental results to define the scope of the transformations and computational studies to explain why this reaction is favored over O–H insertions for reactions with donor/acceptor carbenoids and highly functionalized propargylic alcohols.

## RESULTS AND DISCUSSION

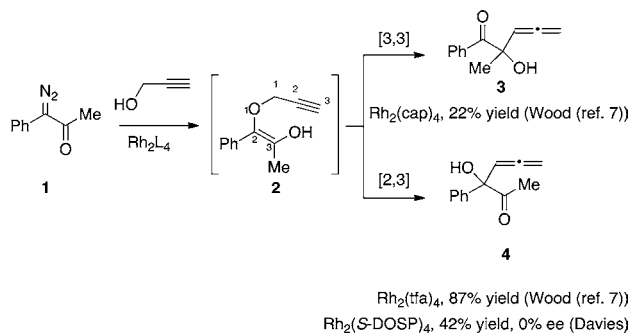
Wood and co-workers have previously explored the reactions of carbenoids with propargylic alcohols using  $\alpha$ -diazoketones as the carbenoid precursors.<sup>8</sup> The reaction of diazoketone **1** with propargyl alcohol generates an alkoxy enol intermediate **2**, which undergoes either a [3,3]-sigmatropic rearrangement to

Received: June 24, 2012

Published: August 27, 2012

give  $\alpha$ -hydroxy allene **3** when the electron-rich catalyst  $\text{Rh}_2(\text{cap})_4$  is used or a [2,3]-sigmatropic rearrangement to give the isomeric  $\alpha$ -hydroxy allene **4** when the electron-deficient catalyst  $\text{Rh}_2(\text{tfa})_4$  is used (Scheme 2). However, as the

### Scheme 2. Reaction of Diazoketones with Propargylic Alcohols



Wood protocol generates **4** via the intermediacy of the planar enol **2**, this mechanism would be expected to preclude the transfer of any asymmetric induction generated during ylide formation into the final product **4**. Indeed, when we replicated this reaction using our standard chiral catalyst,  $\text{Rh}_2(\text{S-DOSP})_4$ , we obtained the  $\alpha$ -hydroxy allene **4** in modest yield with no asymmetric induction.

We hypothesized that enol formation would be suppressed if a diazoester was used instead of a diazoketone as the carbenoid precursor. Therefore, we examined the  $\text{Rh}_2(\text{S-DOSP})_4$ -catalyzed reactions of diazoacetates **5a–d** with a series of functionalized propargylic alcohols **6** (Table 1). The reaction of phenyldiazoacetate **5a** with propargyl alcohol (**6a**) gave none of the allene product (entry 1). Instead, the O–H insertion product **7a** was isolated in 50% yield, and as is typical of rhodium-catalyzed O–H insertions, **7a** was formed with no asymmetric induction. We knew from our studies with allyl alcohols that the [2,3] sigmatropic rearrangement of the oxonium ylide is favored when the allyl group is more highly substituted.<sup>5</sup> The reaction of **5a** with the tertiary propargylic alcohol **6b** did result in the formation of the [2,3]-sigmatropic rearrangement product **8b** in 42% yield and 27% ee (entry 2). The racemic O–H insertion byproduct **7b** was still formed, albeit in diminished yield (12%). Further improvement was

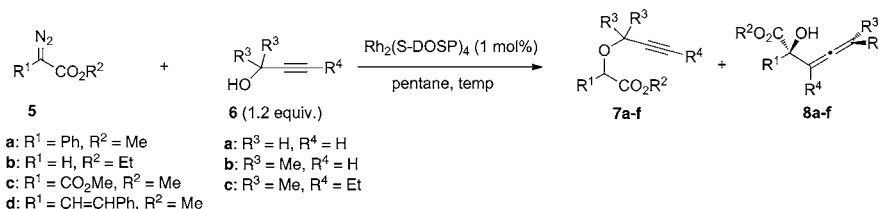
seen when an even more highly substituted propargylic alcohol, 2-methyl-3-hexyn-2-ol (**6c**), was used as the substrate (entry 3). The [2,3]-sigmatropic rearrangement product **8c** was cleanly formed in 61% isolated yield with 79% ee. An increase in asymmetric induction occurred on lowering the reaction temperature to 0 °C, and, under these conditions, compound **8c** was cleanly formed in 85% isolated yield with 85% ee (entry 4).

The competition between allene formation and O–H insertion is highly dependent on the nature of the carbenoids. The reaction of **6c** with ethyl diazoacetate (**5b**) gave only the O–H insertion product **7d** (entry 5). The reaction of **6c** with methyl diazomalonnate (**5c**) gave a 7:1 mixture of [2,3]-sigmatropic rearrangement product **8e** and the O–H insertion product **7e**, with **8e** isolated in 59% yield (entry 6). The most impressive result was obtained from the reaction of **6c** with styryldiazoacetate **5d**. This reaction cleanly formed the [2,3]-sigmatropic rearrangement product **8f**, which was isolated in 74% yield with 96% ee (entry 7). These results indicate that donor/acceptor carbenoids are the best-suited carbenoids for the tandem oxonium ylide formation/[2,3]-sigmatropic rearrangement of propargylic alcohols under these conditions.

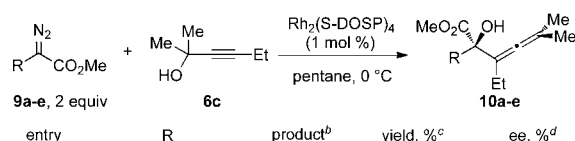
The reactions of **6c** can be extended to a series of styryldiazoacetates **9** (Table 2). Styryldiazoacetates with electron-withdrawing groups such as Br–, CF<sub>3</sub>, and Cl– on the aryl group were tolerated in the reaction, and [2,3]-sigmatropic rearrangement products **10a–e** were formed with good yield and very high levels of enantioselectivity (entries 1–4, 77–85% yield, 85–97% ee). However, the reaction with styryldiazoacetate **9e**, containing electron-donating groups on the aryl ring, gave low yield of **10e** (34%, entry 5), although the enantioselectivity was still high (92% ee). In all of these cases, the O–H insertion product was not observed (ratio of [2,3]-sigmatropic rearrangement/O–H insertion: >20:1).

The reaction was applied to a range of propargylic alcohols **11** as illustrated in Table 3. The styryldiazoacetate **5d** was used as the reference system. The desired [2,3]-sigmatropic rearrangement products were obtained with uniformly excellent levels of enantioselectivity. In all cases, the O–H insertion product was not observed. Alkyl groups (linear or cyclic, entries 1–6), TBS protected alcohols (entries 7–8), and substituents containing phenyl groups (entries 9–12) were all compatible with this reaction. This suggests that the allene formation is a highly favorable process as many of these substrates have

Table 1. Optimization of the Asymmetric Tandem Ylide Formation/[2,3]-Sigmatropic Rearrangement



entry	diazo compound	propargyl alcohols	temp, °C	product (s)	yield of 7, %	ee of 7, %	yield of 8, %	ee of 8, %
1	5a	6a	23	7a	50	0	<5	
2	5a	6b	23	7b, 8b	12	0	42	27
3	5a	6c	23	8c	<5		61	79
4	5a	3c	0	8c	<5		85	85
5	5b	3c	0	7d	27	0	<5	
6	5c	3c	0	7e, 8e	~10		59	
7	5d	3c	0	8f	<5		74	96

**Table 2.** Reaction of Styryldiazoacetate **9a–e** with 2-Methyl-3-hexyn-2-ol (**6c**)<sup>a</sup>

entry	R	product <sup>b</sup>	yield, % <sup>c</sup>	ee, % <sup>d</sup>
1		<b>10a</b>	81	97
2		<b>10b</b>	85	96
3		<b>10c</b>	81	85
4		<b>10d</b>	77	96
5		<b>10e</b>	34	92

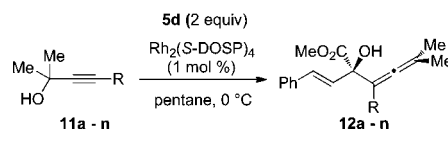
<sup>a</sup>Standard reaction conditions: **9** (1.0 mmol, 2.0 equiv) in pentane (9 mL) with the minimum amount of toluene required for solubilization was added to a solution of **6c** (0.5 mmol, 1.0 equiv) and Rh<sub>2</sub>(S-DOSP)<sub>4</sub> (0.005 mmol, 1 mol %) in pentane (1 mL) over 1.5 h at 0 °C. <sup>b</sup><sup>1</sup>H NMR of the crude reaction mixtures revealed that the [2,3]-sigmatropic rearrangement/O–H insertion ratio in each case was >20:1. <sup>c</sup>Isolated yield of **10a–e**. <sup>d</sup>Determined by chiral HPLC.

potentially active sites for C–H functionalization or cyclopropanation. Alcohols with very bulky R groups, such as *t*-butyl and trimethylsilyl, however, gave only moderate yields of product (entries 13,14). The absolute configuration of **12e** was determined by X-ray crystallography (see the Supporting Information), and the absolute configuration of the other products was assigned by analogy.

The reaction could also be extended to propargylic alcohols, **13a–c**, containing cyclic subunits as shown in Scheme 3. In each case, the allenics **14a–c** were cleanly formed in 69–85% yield with 88–95% ee.

The reactions described so far generate allenics with a single stereogenic center. To challenge the reaction further, substrates were examined in which two new stereogenic centers would be generated (Table 4). It was envisioned that the size difference between methyl and the second alkyl group, *c*-hexyl, *i*-Pr, or *t*-Bu, could lead to kinetic resolution of chiral racemic propargylic alcohols. Several examples of kinetic resolution are known in carbenoid chemistry,<sup>9</sup> but none of these examples involve the reaction of carbenoids with alcohols. The reaction of racemic alcohol **15a** with styryldiazoacetate **5d** gave moderate diastereocontrol, and the allenic alcohols **16a** and **17a** were formed in 6.1:1 dr and in a combined yield of 49% (entry 1).<sup>10</sup> The major diastereomer **16a** was formed in 88% ee. Under these reaction conditions, **15a** was recovered in 35% yield and was found to be enriched to 95% ee, confirming that we were indeed observing a kinetic resolution of the starting material. Similar results were obtained for the *i*-Pr and *t*-Bu derivatives, **15b** and **15c** (entries 2 and 3).

To further understand the stereochemical outcome with chiral alcohols, we carried out the reaction with enantiomerically enriched alcohols, (*R*) and (*S*)-**15a**, which were obtained by conducting the reaction of racemic **15a** with **5d** on a larger scale (5 mmol) with either Rh<sub>2</sub>(S-DOSP)<sub>4</sub> or Rh<sub>2</sub>(R-DOSP)<sub>4</sub>

**Table 3.** Reaction of Styryldiazoacetate **5d** with Alcohols **11a–n**<sup>a</sup>

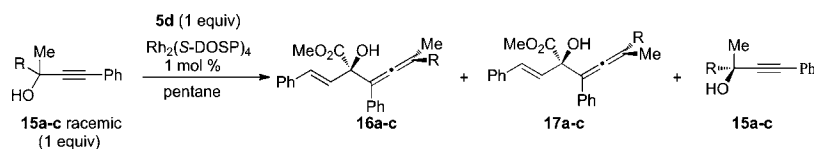
entry	R	product <sup>b</sup>	yield, % <sup>c</sup>	ee, % <sup>d</sup>
1	CH <sub>3</sub>	<b>12a</b>	77	96
2	<i>n</i> -C <sub>4</sub> H <sub>9</sub>	<b>12b</b>	86	95
3	<i>n</i> -C <sub>10</sub> H <sub>21</sub>	<b>12c</b>	88	96
4		<b>12d</b>	60	92
5		<b>12e</b>	78	98
6		<b>12f</b>	51	97
7		<b>12g</b>	66	90
8		<b>12h</b>	84	96
9		<b>12i</b>	72	97
10		<b>12j</b>	59	94
11		<b>12k</b>	44	92
12		<b>12l</b>	79	95
13		<b>12m</b>	44	96
14		<b>12n</b>	37	94

<sup>a</sup>The reaction conditions described in Table 2 were used. <sup>b</sup><sup>1</sup>H NMR of the crude reaction mixtures revealed that the [2,3]-sigmatropic rearrangement/O–H insertion ratio in each case was >20:1. <sup>c</sup>Isolated yield of **12a–n**. <sup>d</sup>Determined by chiral HPLC.

**Scheme 3.** Formation of Cyclic Allenics **14**

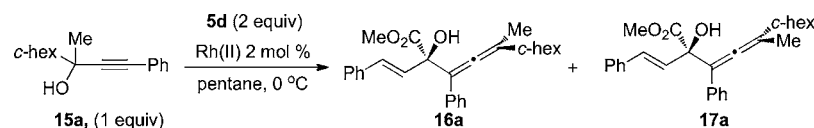
n	product	yield, %	ee, %
1	<b>14a</b>	69	88
2	<b>14b</b>	85	94
3	<b>14c</b>	82	95

as the catalyst (see the Supporting Information for details). The results of the reactions of styryldiazoacetate **5d** with enantiomerically enriched **15a** are summarized in Table 5. We observed distinct matched/mismatched reactions. For example, the reaction of (*S*)-**15a** with Rh<sub>2</sub>(S-DOSP)<sub>4</sub> or (*R*)-**15a** with Rh<sub>2</sub>(R-DOSP)<sub>4</sub> resulted in the formation of **16a** in high yield with extremely high diastereo- and enantioselectivity (>20:1 dr, >99% ee, Table 5, entries 1 and 3). In the mismatch situation, (*S*)-**15a** with Rh<sub>2</sub>(R-DOSP)<sub>4</sub> or (*R*)-**15a** with Rh<sub>2</sub>(S-DOSP)<sub>4</sub>, much inferior results were obtained (Table 5, entries 2 and 4). The diastereoselectivity was low (~2:1 dr), favoring **17a**. Although compound **17a** was formed in 96–97% ee, the

Table 4. Reaction of Styryldiazoacetate **5d** with Racemic Alcohols **15**<sup>a</sup>

entry	alcohol	R	16:17 ratio <sup>b</sup>	yield of <b>16</b> + <b>17</b> , % <sup>c</sup>	ee of <b>16</b> , % <sup>d</sup> (configuration)	yield of recovered <b>15</b> , % <sup>c</sup>	ee of <b>15</b> , % <sup>d</sup> (configuration)
1	<b>15a</b>	<i>c</i> -hex	6.1:1	49	88 (2 <i>R</i> , 4 <i>S</i> )	35	95 ( <i>R</i> )
2	<b>15b</b>	<i>i</i> -Pr	3.3:1	47	93 (2 <i>R</i> , 4 <i>S</i> )	36	81 ( <i>R</i> )
3	<b>15c</b>	<i>t</i> -Bu	6.7:1	50	93 (2 <i>R</i> , 4 <i>S</i> )	42	77( <i>R</i> )

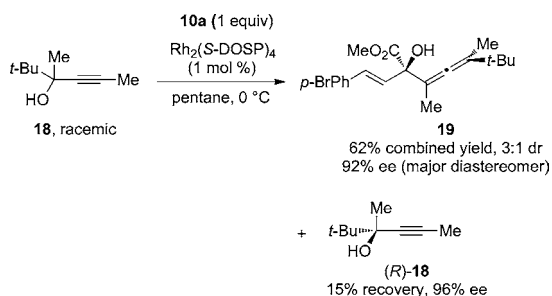
<sup>a</sup>Reactions were performed using the standard conditions described in Table 2. <sup>b</sup>Determined by <sup>1</sup>H NMR of the crude reaction mixture. <sup>c</sup>Isolated yield. <sup>d</sup>Determined by chiral HPLC.

Table 5. Reaction of Styryldiazoacetate **5d** with (*R*)- and (*S*)-**15a**

entry	alcohol	Rh(II) catalyst	16a:17a <sup>b</sup>	yield, %	ee of <b>16a</b> , % <sup>c</sup>	ee of <b>17a</b> , %
1	( <i>S</i> )- <b>15a</b> (95% ee)	Rh <sub>2</sub> ( <i>S</i> -DOSP) <sub>4</sub>	>20:1	70 <sup>c</sup>	>99	
2	( <i>S</i> )- <b>15a</b> (95% ee)	Rh <sub>2</sub> ( <i>R</i> -DOSP) <sub>4</sub>	1:1.7	42 <sup>d</sup>	51	-97 <sup>f</sup>
3	( <i>R</i> )- <b>15a</b> (96% ee)	Rh <sub>2</sub> ( <i>R</i> -DOSP) <sub>4</sub>	>20:1	79 <sup>c</sup>	>-99 <sup>f</sup>	
4	( <i>R</i> )- <b>15a</b> (96% ee)	Rh <sub>2</sub> ( <i>S</i> -DOSP) <sub>4</sub>	1:2.1	39 <sup>d</sup>	-59 <sup>f</sup>	96

<sup>a</sup>Reactions were performed with Rh<sub>2</sub>(*S*- or *R*-DOSP)<sub>4</sub> under the standard reactions conditions described in Table 2. <sup>b</sup>Determined by <sup>1</sup>H NMR of the crude reaction mixture. <sup>c</sup>Isolated yield of **16a**. <sup>d</sup>Combined yield of (**16a** + **17a**). <sup>e</sup>Determined by chiral HPLC. <sup>f</sup>“Negative” value signifies the opposite enantiomeric series.

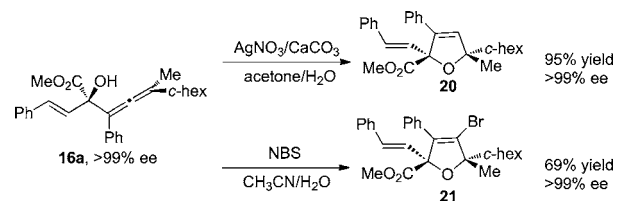
formation of the minor diastereomer was less enantioselective (51–59% ee). Compound **16a** from the reaction of (*S*)-**15a** and Rh<sub>2</sub>(*S*-DOSP)<sub>4</sub> (entry 1, >99% ee) was recrystallized from cold hexanes, and the resulting crystals were analyzed by X-ray crystallography. The configuration of the tertiary alcohol in **16a** was determined by X-ray crystallography and agrees with the determined absolute configuration of **12e**. The configuration of the allene component of **16** is (*S*) (see the Supporting Information). The configurations of **16b** and **16c** were assigned by analogy to **16a**. A similar kinetic resolution was conducted with the racemic alcohol **18** (Scheme 4). The recovered alcohol

Scheme 4. Kinetic Resolution of **18**

from the Rh<sub>2</sub>(*S*-DOSP)<sub>4</sub>-catalyzed reaction was assigned as (*R*)-**18** from comparison of its optical rotation with literature values (recovered (*R*)-**18**: 96% ee, [ $\alpha$ ]<sub>D</sub><sup>20</sup>: +1.94° (*c* 6.03, Et<sub>2</sub>O); lit. +1.44° (*c* 6.03, Et<sub>2</sub>O)).<sup>11</sup> On the assumption that the same sense of kinetic resolution would be observed with the propargylic alcohols **15** and **18**, the recovered alcohols **15** from the Rh<sub>2</sub>(*S*-DOSP)<sub>4</sub>-catalyzed reactions were assigned as (*R*) configurations.

The stereoselective conversion of chiral allenic alcohol into 2,5-dihydrofuran has been extensively studied,<sup>12,13</sup> and also successfully applied to the total synthesis of complex natural products such as amphidinolide X and Y,<sup>14</sup> and boivinianin B.<sup>15</sup> The highly substituted allenic alcohol **16a** can also be easily transformed into various 2,5-dihydrofuran derivatives with excellent chirality transfer (Scheme 5). Treatment of **16a** with

Scheme 5. Cyclization of Allenes to Dihydrofurans



AgNO<sub>3</sub> and CaCO<sub>3</sub> provided dihydrofuran **20**, while treatment with NBS provided the bromodihydrofuran **21** with two quaternary stereogenic centers at the 2,5-positions of the dihydrofuran. Both products were formed in good yield and >99% ee.

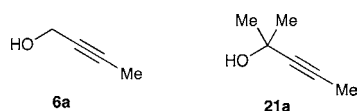
## MECHANISTIC DFT STUDIES

The allene formation is believed to occur via ylide formation, followed by a [2,3]-sigmatropic rearrangement of the rhodium-associated ylide. Normally, racemic O–H insertion occurs readily in the presence of alcohols with most rhodium carbenoids, and, indeed, this is observed with simple propargylic alcohols in this study. Computational studies on the O–H insertion mechanism of rhodium carbenoids with water have been reported,<sup>4,16</sup> and the reaction preferentially goes through a pathway involving a free enol, thereby losing



any asymmetric induction that may be generated during ylide formation.<sup>4</sup> Considering the high levels of asymmetric induction observed in the tandem oxonium ylide formation/[2,3]-sigmatropic rearrangement, a more detailed mechanistic investigation of the [2,3]-sigmatropic rearrangement was warranted. These studies could shed light on the following vital questions: (1) What are the factors that govern partitioning between O–H insertion and the [2,3]-sigmatropic rearrangement? (2) Why is [2,3]-sigmatropic rearrangement so strongly favored with donor/acceptor carbenoids and more highly functionalized propargylic alcohols? (3) Why is ylide formation so highly enantioselective? (4) What is the mechanism of the chirality transfer during the [2,3]-sigmatropic rearrangement?

For these purposes, we conducted detailed DFT calculations on ylide formation followed by either the O–H insertion or the [2,3]-sigmatropic rearrangement pathways.<sup>17</sup> The study was conducted on an unsubstituted vinylcarbenoid reacting with both the primary propargylic alcohol **6a**, which favors O–H insertion, and the highly substituted propargylic alcohol **21a**, which favors the [2,3]-sigmatropic rearrangement.



The calculated<sup>17,18</sup> energies presented below were referenced to the reactants, that is, VC-I plus **21a** (**6a**), and presented as  $\Delta H/\Delta G(\Delta G_{\text{sol}})$ , where  $\Delta H$  and  $\Delta G$  are the gas-phase enthalpy and Gibbs free energy, respectively.  $\Delta G_{\text{sol}}$  is calculated as  $\Delta G_{\text{s}} + [\Delta G - \Delta E]$ , where  $\Delta G_{\text{s}}$  is the PCM calculated free energy in solution, and  $\Delta E$  is the gas-phase total energy.

**Reaction of VC-I with 21a.** A summary of the calculated reaction pathways between propargylic alcohol **21a** and

vinylcarbenoid VC-I, formed through nitrogen extrusion reaction between  $\text{Rh}_2(\text{O}_2\text{CH})_4$  and methyl 2-diazobutanoate, is illustrated in Figure 1. The reaction starts with the formation of a prereaction complex PC-I, where propargylic alcohol **21a** and vinylcarbenoid VC-I are bound via two weak interactions: the  $(\text{O}^2 \cdots \text{H}^1)$  hydrogen bonding with  $d(\text{O}^2 \cdots \text{H}^1) = 2.316 \text{ \AA}$  and  $(\text{O}^1 \cdots \text{C}^1)$  bonding with  $d(\text{O}^1 \cdots \text{C}^1) = 2.884 \text{ \AA}$ . The weak  $(\text{O}^1 \cdots \text{C}^1)$  bonding in PC-I did not impact the hybridization state of the reactive  $\text{sp}^2$ -hybridized carbenoid carbon (impr. angle =  $5^\circ$ ). From PC-I, the reaction proceeds via the transition state TS-I, where the  $(\text{O}^2 \cdots \text{H}^1)$  and  $(\text{O}^1 \cdots \text{C}^1)$  bonding became stronger (with  $d(\text{O}^2 \cdots \text{H}^1) = 1.917 \text{ \AA}$  and  $d(\text{O}^1 \cdots \text{C}^1) = 1.966 \text{ \AA}$ ), and the pyramidalization of  $\text{C}^1$  is more enhanced (impr. angle =  $22^\circ$ ). This two-point interaction, that is, the  $(\text{O}^2 \cdots \text{H}^1)$  and  $(\text{O}^1 \cdots \text{C}^1)$  bonding, nascent in prereaction complex PC-I and developed via transition state TS-I, defines the orientation of the allylic alcohol as it approaches the carbenoid and is likely to be a crucial factor that impacts the high asymmetric induction in this chemistry. A similar type of two-point interaction, involving hydrogen bonding to the carboxylate ligands, has been observed in computational studies on rhodium-catalyzed cyclopropanation of internal alkynes.<sup>19</sup>

The calculated relative energy of TS-I is  $\Delta H/\Delta G(\Delta G_{\text{sol}}) = -5.8/10.2(12.0)$  kcal/mol. Intrinsic reaction coordinate (IRC) calculations confirm that TS-I connects PC-I with ylide YL-I intermediate: the calculated energy of singlet ground state of ylide intermediate YL-I is  $-12.8/2.7(3.6)$  kcal/mol relative to reactants. The ylide YL-I has a reinforced hydrogen ( $d(\text{O}^2 \cdots \text{H}^1) = 1.705 \text{ \AA}$ ) and C–O bonding ( $d(\text{O}^1 \cdots \text{C}^1) = 1.483 \text{ \AA}$ ). The carbenoid center of YL-I has strongly pyramidalized (impr. angle =  $43^\circ$ ). One should mention that the ground electronic states of PC-I, TS-I, and YL-I are the closed-shell singlet states. Their triplet states are significantly higher in energy (see below).

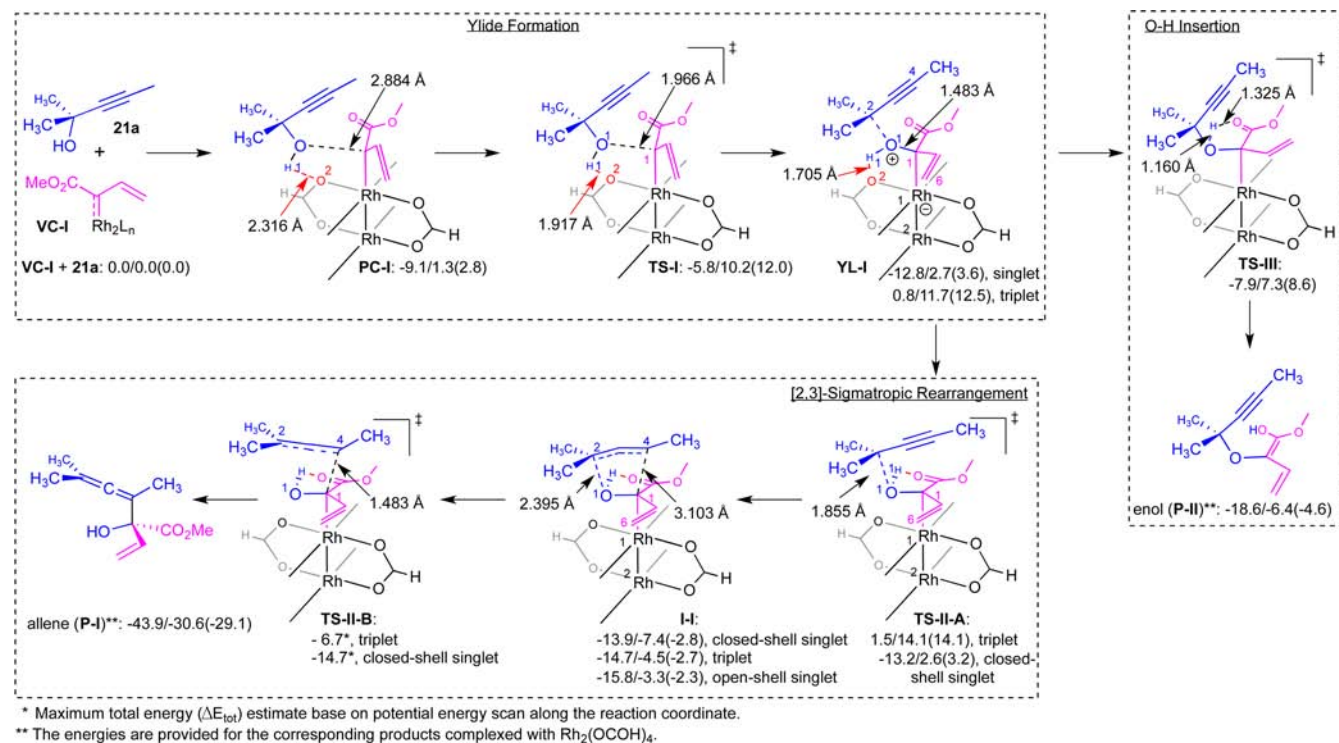


Figure 1. Mechanism of the reaction of vinylcarbene VC-I with alcohol **21a**.

After formation of the **YL-I** intermediate, the reaction may proceed via either of two distinct pathways: (1) the [2,3]-sigmatropic rearrangement or (2) proton transfer to the carbonyl group ( $O^1-H^1$  insertion). The diazo compound and the propargylic alcohol are the control elements for which pathway will occur with donor/acceptor carbenoids and highly substituted propargylic alcohols strongly favoring the [2,3]-sigmatropic rearrangement. The [2,3]-sigmatropic rearrangement, as shown in the literature, may proceed via a concerted pathway or in a stepwise fashion, involving either homolytic or heterolytic bond cleavage/recombination mechanisms.<sup>20</sup> Calculations show that singlet **YL-I** undergoes heterolytic  $C^2-O^1$  bond cleavage with almost no energy barrier at the singlet transition state **TS-II-A**: the energy of the closed-shell singlet **TS-II-A** is calculated to be  $-13.2/2.6(3.2)$  kcal/mol relative to singlet reactants. IRC calculations confirm that singlet **TS-II-A** connects singlet **YL-I** with the closed-shell singlet intermediate **I-I**, which is  $-13.9/-7.4(-2.8)$  kcal/mol lower in energy than reactants.

The homolytic  $C^2-O^1$  bond cleavage of **YL-I** proceeds via a triplet **TS-II-A** transition state, which is calculated to be  $1.5/14.1(14.1)$  kcal/mol higher in energy than singlet state reactants, that is, **VC-I** + **21a**. These values are over 10 kcal/mol higher than those for the singlet state **TS-II-A**. IRC calculations confirm that triplet **TS-II-A** connects the triplet **YL-I** (which is calculated to be  $13.6/9.0(8.9)$  kcal/mol higher than its singlet ground state) with the triplet intermediate **I-I**. The energy barrier at triplet **TS-II-A**, calculated from the triplet **YL-I**, is found to be only  $0.7/2.4(1.6)$  kcal/mol. Unlike the prereaction complex **YL-I** and transition state **TS-II-A**, intermediate **I-I** has close-lying singlet and triplet states: closed-shell singlet, open-shell singlet, and triplet states with energies of  $-13.9/-7.4(-2.8)$ ,  $-15.8/-3.3(-2.3)$ , and  $-14.7/-4.5(-2.7)$  kcal/mol, respectively.

The data discussed in the preceding paragraph suggest that the reaction involves the closed-shell singlet states of **YL-I** and **TS-II-A**, because of calculated large singlet–triplet energy gaps in these systems. However, the electronic structure of the intermediate **I-I** is less obvious, because its closed-shell singlet, open-shell singlet, and triplet states are close in energy. Thus, one should apply DFT-based methods to **I-I** with caution. In this case, the multideterminant approaches, such as CASSCF and MRD-CI, are required to identify the degree of radical character in the total wave function of **I-I**. However, such methods have a significantly higher computational cost than DFT, and their use is beyond the scope of the present work.

Thus, we conclude that the reaction **YL-I**  $\rightarrow$  **TS-II-A**  $\rightarrow$  **I-I** starts from the closed-shell singlet prereaction complex **YL-I**, proceeds via closed-shell singlet (“reactant-like”) transition state **TS-II-A**, and leads to intermediate **I-I** with several lower-lying electronic states. In other words, this reaction proceeds via heterolytic  $C^2-O^1$  bond cleavage mechanism, but leads to product with a significant diradical (i.e., homolytic  $C^2-O^1$  bond cleavage) character. To estimate the region of the potential energy surface (PES) where the singlet and triplet states may cross, we did scan it for all three states (closed-shell singlet, open-shell singlet, and triplet states) starting from the intermediate **I-I** by fixing of  $C^2-O^1$  (reaction coordinate leading back to the starting material) bond distances but optimizing all other parameters. These calculations clearly indicate that closed-shell and open-shell states cross in the vicinity of intermediate **I-I**. Thus, in this simplified model

system, the transition state **TS-II-A** has no significant radical character.

The performed Mulliken spin density analyses are consistent with the above-presented findings. Indeed, in the triplet state of **YL-I**, two  $\alpha$ -spins are located, mostly on the  $Rh^1$  [1.15 |e|],  $Rh^2$  [0.49 |e|], and  $C^6$  [0.20 |e|] centers. The spin density distribution in the triplet state transition state **TS-II-A** is very similar to that for the prereaction complex **YL-I**:  $Rh^1$  [1.17 |e|],  $Rh^2$  [0.43 |e|], and  $C^6$  [0.22 |e|]. However, in case of intermediate **I-I**, the largest portion ( $\sim 1.15 e$ ) of the two  $\alpha$ -spins is located on substrate **21a**: in triplet **I-I** spin density is distributed as  $Rh^2$  [0.29 |e|],  $C^1$  [0.29 |e|],  $C^2$  [0.65 |e|],  $C^4$  [0.51 |e|], and  $C^6$  [0.47 |e|]. Thus, the electronic structure of transition state **TS-II-A** is very much “reactant-like”. However, the progression of the reaction via **YL-I**  $\rightarrow$  **TS-II-A**  $\rightarrow$  **I-I** is accompanied by significant spin buildup at the reactive (at the next stage of the reaction) carbon centers ( $C^1$ ,  $C^2$ , and  $C^4$ ) that facilitates the allene formation ( $C^4-C^1$  formation) via a radical coupling mechanism. It is expected that having alkyl substituents on the propargylic alcohol and electron-donating groups on the carbenoid fragment will further promote spin buildup on the reactive carbon centers and stabilize transition state **TS-II-A** associated with the [2,3]-sigmatropic rearrangement by making its electronic structure more “product-like”. This conclusion is in excellent agreement with our experimental findings presented in Table 1. Neither the reaction of ethyl diazoacetate with a trialkylated propargylic alcohol (entry 5) nor the reaction of methyl phenyldiazoacetate with the unsubstituted propargylic alcohol (entry 1) give any of the [2,3]-sigmatropic rearrangement products because only one radical center in the diradical intermediate would be stabilized. In contrast, when a donor/acceptor carbenoid is reacted with a highly substituted propargylic alcohol, as in entries 3 and 7, exclusive formation of the 2,3-sigmatropic rearrangement products is observed. In these cases, both of the radical centers are stabilized. These conclusions also help rationalize the similar product distributions trends seen in the reaction of allyl alcohols with donor/acceptor carbenoids.<sup>5a</sup>

One should note that we were not able to calculate the exact location of the closed-shell singlet and triplet states of the allene formation **TS-II-B** on the potential energy surface of the reaction. Instead, we estimated the upper limit of energy barriers associated with these transition states by scanning PESs of the reactions: they are  $\Delta E_{tot} = -14.7$  and  $-6.7$  kcal/mol, respectively. Both states of **TS-II-B** are lower in total energy ( $\Delta E_{tot}$ ) than **TS-II-A** by  $-0.1$  and  $-6.0$  kcal/mol, respectively, but higher than **I-I** by  $1.7$  and  $9.4$  kcal/mol, respectively. IRC calculations indicate that the transition state **TS-II-B** connects **I-I** with the allene product **P-I** as a complex with  $Rh_2(OCOH)_4$ .

Thus, the above presented findings indicate that after formation of **YL-I**, which requires a  $3.3/10.2(12.0)$  kcal/mol barrier, the overall [2,3]-sigmatropic rearrangement occurs with no significant energy barrier. The mechanism predicts that *R*-face attack on the carbenoid would lead to the *R*-configuration of the quaternary stereocenter in **P-I**, and this prediction is consistent with experimental observations for reactions with  $Rh_2(S-DOSP)_4$ .<sup>1b</sup>

The alternative pathway from **YL-I** is proton transfer (to the carbonyl group) that leads to enol **P-II** and proceeds via transition state, **TS-III**. Later, enol **P-II** could tautomerize to the formal  $O-H$  insertion product. All reactants, transition states, and products of this reaction have a well-defined closed-

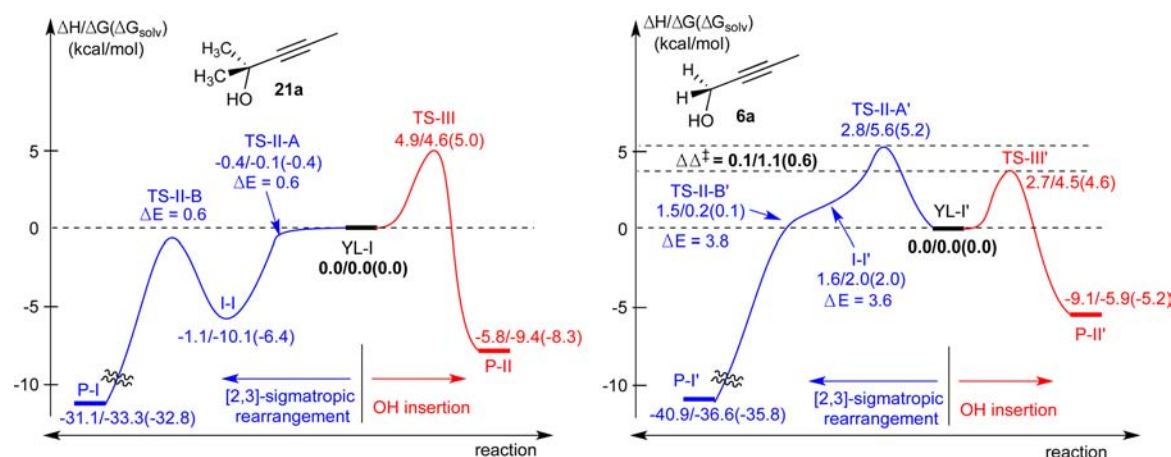


**Figure 2.** Comparison of the important steps of the O–H insertion and [2,3]-sigmatropic rearrangement pathways for alcohols **6a** and **21a**, respectively. Schemes are scaled to  $\Delta G_{\text{solv}}$ . All energetics presented in this figure are for the singlet states of the intermediates, transition states, and products.

shell singlet state; that is, they have no radical character. One should mention that IRC calculations confirm that **TS-III** connects **P-II** with **YL-I**. Formation of the enol explains why O–H insertion products are racemic in Rh(II)-catalyzed processes. The involvement of enol intermediates in the rhodium-catalyzed O–H insertion is in agreement with previous theoretical calculations on O–H insertion.<sup>4</sup>

The formation of allene **P-I** versus O–H insertion is controlled by the relative energetics of **TS-II-A** and **TS-III**, respectively. As seen in Figure 2 (left), the calculated insignificant energy barrier for [2,3]-sigmatropic rearrangement for the ylide derived from **21a** makes it favorable over the O–H insertion, which requires a +4.9/4.6(5.0) kcal/mol energy barrier.

We also calculated reaction of **VC-I** with the nonsubstituted propargylic alcohol **6a** (Figure 2, right). The overall reaction pathways for **6a** are similar to **21a** (see the Supporting Information). The reaction of alcohol **6a** and **VC-I** forms **PC-I'** that rearranges to ylide **YL-I'** via the transition state **TS-I'**. The required energy barrier for this process is 4.1/8.2(8.5) kcal/mol. The intermediate **YL-I'** undergoes either O<sup>1</sup>–H<sup>1</sup> insertion via transition state **TS-III'** to give enol product **P-II'**, or [2,3]-sigmatropic pathway via the transition state **TS-II-A'** to give intermediate **I-I'**. The associated barriers for O<sup>1</sup>–H<sup>1</sup> insertion and [2,3]-sigmatropic rearrangement are calculated to be 2.7/4.5(4.6) and 2.8/5.6(5.3) kcal/mol, respectively. Comparison of these barriers for **6a** with those reported above for **21a** shows that the lack of two methyl groups did not introduce a significant change in the free energy barrier of the O<sup>1</sup>–H<sup>1</sup> insertion, whereas it significantly increased the energy barrier for the C<sup>2</sup>–O<sup>1</sup> bond cleavage step of [2,3]-sigmatropic rearrangement. Intermediate **I-I'** possessed an ambiguous electronic structure similar to that of **I-I**; however, this intermediate became less important because the barriers at the transition state **TS-II-A'** leading to this intermediate cannot compete with that at **TS-III'** leading to enol product **P-II'**.

## CONCLUSIONS

In summary, we have discovered that the reaction of carbenoids with propargylic alcohols can lead to a tandem oxonium ylide formation/[2,3]-sigmatropic rearrangement, instead of O–H insertion. The reaction is favored when donor/acceptor carbenoids and highly functionalized propargylic alcohols are

used as substrates. A predictive model was developed on the basis of a detailed computational study that explains the factors that control the partitioning between the [2,3]-sigmatropic rearrangement and O–H insertion. The model also rationalizes the diastereoselectivity observed in these reactions. The most distinctive aspects of the model include a two-point binding during ylide formation and the diradical character of the [2,3]-sigmatropic rearrangement.

## ASSOCIATED CONTENT

### Supporting Information

Synthetic details, computational details, and spectral data. This material is available free of charge via the Internet at <http://pubs.acs.org>.

## AUTHOR INFORMATION

### Corresponding Author

[hmdavie@emory.edu](mailto:hmdavie@emory.edu)

### Notes

The authors declare no competing financial interest.

## ACKNOWLEDGMENTS

This material is based on work supported by the National Institutes of Health (GM099142). We thank Dr. Ken Hardcastle for the X-ray crystallographic structural determination. We gratefully acknowledge NSF-MRI-R2 grant (CHE-0958205) and the use of the Cherry Emerson Center for Scientific Computation. We also acknowledge the University at Buffalo's Center for Computational Research for technical support.

## REFERENCES

- (1) (a) Doyle, M. P.; McKervey, M. A.; Ye, T. *Modern Catalytic Methods for Organic Synthesis with Diazo Compounds: From Cyclopropanes to Ylide*; Wiley: New York, 1998. (b) Davies, H. M. L.; Beckwith, R. E. J. *Chem. Rev.* **2003**, *103*, 2861–2904. (c) Moody, C. J. *Angew. Chem., Int. Ed.* **2007**, *46*, 9148–9150. (d) Zhang, Z.; Wang, J. *Tetrahedron* **2008**, *64*, 6577–6605. (e) Davies, H. M. L.; Manning, J. R. *Nature* **2008**, *451*, 417–424. (f) Doyle, M. P.; Duffy, R.; Ratnikov, M.; Zhou, L. *Chem. Rev.* **2010**, *110*, 704–724.
- (2) (a) Miller, D. J.; Moody, C. J. *Tetrahedron* **1995**, *51*, 10811–10843. (b) Zhu, S. F.; Zhou, Q. L. *Acc. Chem. Res.* **2012**, ASAP (DOI: 10.1021/ar300051u).



(3) (a) Maier, T. C.; Fu, G. C. *J. Am. Chem. Soc.* **2006**, *128*, 4594–4595. (b) Chen, C.; Zhu, S. F.; Liu, B.; Wang, L.-X.; Zhou, Q.-L. *J. Am. Chem. Soc.* **2007**, *129*, 12616–12617. (c) Zhu, S.-F.; Chen, C.; Zhou, Q.-L. *Angew. Chem., Int. Ed.* **2008**, *47*, 932–934. (d) Zhu, S.-F.; Song, X.-G.; Li, Y.; Cai, Y.; Zhou, Q.-L. *J. Am. Chem. Soc.* **2010**, *132*, 16374–16376.

(4) For a computational study regarding the difference between copper(I) and dirhodium(II) complexes in catalytic asymmetric O—H insertion reactions, see: Liang, Y.; Zhou, H.; Yu, Z.-X. *J. Am. Chem. Soc.* **2009**, *131*, 17783–17785.

(5) (a) Li, Z.; Davies, H. M. L. *J. Am. Chem. Soc.* **2010**, *132*, 396–401. (b) Parr, B. T.; Li, Z.; Davies, H. M. L. *Chem. Sci.* **2011**, *2*, 2378–2382. (c) Li, Z.; Parr, B.; Davies, H. M. L. *J. Am. Chem. Soc.* **2012**, *134*, 10942–10946.

(6) For representative examples of donor/acceptor carbenoids and their rich chemistry, see refs 1b, 1e, and: (a) Davies, H. M. L.; Denton, J. R. *Chem. Soc. Rev.* **2009**, *38*, 3061–3071. (b) Morton, D.; Davies, H. M. L. *Chem. Soc. Rev.* **2011**, *40*, 1857–1869.

(7) For reviews on the asymmetric synthesis of allenes, see: (a) Miesch, M. *Synthesis* **2004**, 746–752. (b) Ogasawara, M. *Tetrahedron: Asymmetry* **2009**, *20*, 259–271. (c) Yu, S.; Ma, S. *Angew. Chem., Int. Ed.* **2012**, *51*, 3074–3112.

(8) Moniz, G. A.; Wood, J. L. *J. Am. Chem. Soc.* **2001**, *123*, 5095–5097.

(9) For examples of matched/mismatched reactions in the rhodium carbenoid field, see: (a) Martin, S. F.; Spaller, M. R.; Liras, S.; Hartmann, B. *J. Am. Chem. Soc.* **1994**, *116*, 4493–4494. (b) Doyle, M. P.; Dyatkin, A. B.; Kalinin, A. V.; Ruppert, D. A.; Martin, S. F.; Spaller, M. R.; Liras, S. *J. Am. Chem. Soc.* **1995**, *117*, 11021–11022. (c) Doyle, M. P.; Kalinin, A. V.; Ene, D. G. *J. Am. Chem. Soc.* **1996**, *118*, 8837–8846. (d) Davies, H. M. L.; Venkataramani, C.; Hansen, T.; Hopper, D. W. *J. Am. Chem. Soc.* **2003**, *125*, 6462–6468. (e) Davies, H. M. L.; Walji, A. M. *Angew. Chem., Int. Ed.* **2005**, *44*, 1733–1735. (f) Nadeau, E.; Ventura, D. L.; Brekan, J. A.; Davies, H. M. L. *J. Org. Chem.* **2010**, *75*, 1927–1939. (g) Lian, Y.; Miller, L. C.; Born, S.; Sarpong, R.; Davies, H. M. L. *J. Am. Chem. Soc.* **2010**, *132*, 12422–12425.

(10) The absolute configuration of the allene moiety in compound **17a-c** was assigned on the assumption that the catalyst has a controlling effect on the tertiary alcohol stereogenic center in these compounds. For a relevant discussion, see ref 5a.

(11) Damm, L. G.; Hartshorn, M. P.; Vaughan, J. *Aust. J. Chem.* **1976**, *29*, 1017–1021.

(12) For representative examples of the enantioselective synthesis of  $\alpha$ -allenic alcohols containing a secondary alcohol stereogenic center, see: (a) Corey, E. J.; Yu, C.-M.; Lee, D.-H. *J. Am. Chem. Soc.* **1990**, *112*, 878–879. (b) Brown, H. C.; Khire, U. R.; Narla, G. *J. Org. Chem.* **1995**, *60*, 8130–8131. (c) Marshall, J. A.; Adams, N. D. *J. Org. Chem.* **1997**, *62*, 8976–8977. (d) Yu, C.-M.; Yoon, S.-K.; Baek, K.; Lee, J.-Y. *Angew. Chem., Int. Ed.* **1998**, *37*, 2392–2395. (e) Furstner, A.; Mendez, M. *Angew. Chem., Int. Ed.* **2003**, *42*, 5355–5357. (f) Xu, D.; Li, Z.; Ma, S. *Tetrahedron: Asymmetry* **2003**, *14*, 3657–3666. (g) Inoue, M.; Nakada, M. *Angew. Chem., Int. Ed.* **2006**, *45*, 252–255. (h) Xia, G.; Yamamoto, H. *J. Am. Chem. Soc.* **2007**, *129*, 496–497. (i) Miura, T.; Shimada, M.; Ku, S.-Y.; Tamai, T.; Murakami, M. *Angew. Chem., Int. Ed.* **2007**, *46*, 7101–7103. (j) Li, J.; Kong, W.; Fu, C.; Ma, S. *J. Org. Chem.* **2009**, *74*, 5104–5106.

(13) (a) Marshall, J. A.; Pinney, K. G. *J. Org. Chem.* **1993**, *58*, 7180–7184. (b) Marshall, J. A.; Bartley, G. S. *J. Org. Chem.* **1994**, *59*, 7169–7171. (c) Krause, N.; Laux, M.; Hoffmann-Roder, A. *Tetrahedron Lett.* **2000**, *41*, 9613–9616. (d) Hoffmann-Roder, A.; Krause, N. *Org. Lett.* **2001**, *3*, 2537–2538. (e) Krause, N.; Hoffmann-Roder, A.; Canisius, J. *Synthesis* **2002**, 1759–1774. (f) Deutsch, C.; Gockel, B.; Hoffmann-Roder, A.; Krause, N. *Synlett* **2007**, 1790–1794. (g) Poonoth, M.; Krause, N. *Adv. Synth. Catal.* **2009**, *351*, 117–122. (h) Li, J.; Kong, W.; Yu, Y.; Fu, C.; Ma, S. *J. Org. Chem.* **2009**, *74*, 8733–8738. (i) Alcaide, B.; Almendros, P.; Martinez del Campo, T.; Quiros, M. T. *Chem.-Eur. J.* **2009**, *15*, 3344–3346.

(14) (a) Lepage, O.; Kattinig, E.; Furstner, A. *J. Am. Chem. Soc.* **2004**, *126*, 15970–15971. (b) Furstner, A.; Kattinig, E.; Lepage, O. *J. Am. Chem. Soc.* **2006**, *128*, 9194–9204.

(15) Miura, T.; Shimada, M.; de Mendoza, P.; Deutsch, C.; Krause, N.; Murakami, M. *J. Org. Chem.* **2009**, *74*, 6050–6054.

(16) Liu, Z.; Liu, J. *Cent. Eur. J. Chem.* **2009**, *8*, 223–228.

(17) Calculations were performed using the Gaussian 09 software package: Frisch, M. J.; et al. *Gaussian 09*, revision A0.2; Gaussian Inc.: Wallingford, CT, 2009. See the Supporting Information for complete reference.

(18) The calculations were conducted at the M06L/[(SDD+4f)<sub>RI</sub>+{6-311+G(d,p)}] level of theory. The optimized structures of the reactants, intermediates, transition states, and products of this reaction were calculated in the gas phase without any symmetry constraints. Solvent effects (*n*-pentane with  $\epsilon = 1.8371$  was used as a solvent) were incorporated by performing single-point energy calculations on the gas-phase-optimized geometries using the PCM polarizable conductor calculation model. For the M06L method, see: Zhao, Y.; Truhlar, D. G. *J. Chem. Phys.* **2006**, *125*, 194101–18. For SDD basis sets and associated effective core potential, see: (a) Kaupp, M.; Schleyer, P. v. R.; Stoll, H.; Preuss, H. *J. Chem. Phys.* **1991**, *94*, 1360. (b) Bergner, A.; M., D.; Kuechle, W.; Stoll, H.; Preuss, H. *Mol. Phys.* **1993**, *80*, 1431. (c) Dolg, M.; S., H.; Preuss, H.; Pitzer, R. M. *J. Phys. Chem.* **1993**, *97*. See also: Hansen, J.; Autschbach, J.; Davies, H. M. L. *J. Org. Chem.* **2009**, *74*, 6555–6563. For PCM method, see: (d) Tomasi, J.; Persico, M. *Chem. Rev.* **1994**, *94*, 2027–2094. (e) Cammi, R.; Tomasi, J. *J. Comput. Chem.* **1995**, *16*, 1449–1458.

(19) (a) Briones, J. F.; Hansen, J. H.; Hardcastle, K.; Autschbach, J.; Davies, H. M. L. *J. Am. Chem. Soc.* **2010**, *132*, 17211–17215. (b) Goto, T.; Takeda, K.; Shimada, N.; Nambu, H.; Anada, M.; Shiro, M.; Ando, K.; Hashimoto, S. *Angew. Chem., Int. Ed.* **2011**, *50*, 6803–6808.

(20) Sigmatropic rearrangements are well known to display both concerted and diradical character in computational studies. For a discussion of this topic, see: Bachrach, S. M. *Computational Organic Chemistry*; John Wiley & Sons, Inc.: Hoboken, NJ, 2007.